Journal of Alloys and Compounds 479 (2009) 237–241

Contents lists available at ScienceDirect

Journal of Alloys and Compounds

journal homepage: www.elsevier.com/locate/jallcom

Isothermal section of the Mg–Al–Mn ternary system at 400 °C

Y.P. Ren, G.W. Qin*, W.L. Pei, H.D. Zhao, Y. Guo, H.X. Li, M. Jiang, S.M. Hao

Key Laboratory for Anisotropy and Texture of Materials (Ministry of Education), Northeastern University, Shenyang 110004, China

ARTICLE INFO

Article history:
Received 16 September 2008
Received in revised form 5 January 2009
Accepted 7 January 2009
Available online 20 January 2009

Keywords:
Mg–Al–Mn system
Phase equilibrium
Solubility
Isothermal section

ABSTRACT

In this work, the equilibrium phase constituents and compositions in the Mg–Al–Mn ternary system at 400 °C were determined through equilibrated alloy method and diffusion couple technique by using scanning electron microscopy (SEM), X-ray diffraction (XRD) and electron probe micro-analyzer (EPMA). The isothermal section in the Mg-rich corner at 400 °C was thus constructed. No ternary compounds were detected in the Mg-rich corner. Therefore, there exist the equilibrium relationships between the α-Mg solid solution and $Mg_{17}Al_{12}$ compound or the other Al–Mn compound phases. The solubility of Mn in the phases α-Mg and $Mg_{17}Al_{12}$ is almost negligible, while the element Mg can slightly dissolve in the compound $Al_{11}Mn_4$. The lattice parameter dependence of α-Mg solid solution on Al content in Mg–Al–Mn system was finally determined by the XRD results.

1. Introduction

AM-series magnesium alloys have been extensively applied in the automotive and aerospace industry due to their sufficiently high strength, good castability and better corrosion [1]. Much work has mainly been focused on micro-alloying, casting technology and formability to improve comprehensive mechanical properties of AM magnesium alloys [2–7], among which one fundamental work is how to modify β-$Mg_{17}Al_{12}$ phase [5–7]. However, little work has been paid attention to the formation and evolution of the Al–Mn intermetallic phases in these alloys up to date [8]. Actually, the Al–Mn phases have close connection with the mechanical properties of the Mg–Al series alloys [9,10]. Moreover, the Al–Mn intermetallic phases can also act as heterogeneous nucleation sites leading to grain refinement [11–13]. However, no agreement has been reached about the refinement mechanism, i.e. the role of the Al_8Mn_5 or ε-AlMn phase [11,12], since the Al–Mn binary phase diagram in the Mn-rich side is not clear at elevated temperatures.

Ma et al. [8] suggested that there exist several kinds of Al–Mn intermetallic phases such as Al_8Mn_5, $Al_{11}Mn_4$, Al_6Mn, $Al_{86}Mn_{14}$ and AlMn in the as cast AM50 magnesium alloy followed by solid solution treatment and aging. However, Medved et al. [6] reported that only the Al_4Mn compound phase exists in the commercial AM50 magnesium alloy. The right understanding of the microstructural constituents in the AM series alloys can not be obtained, since the phase diagram of the Mg-rich corner in the Mg–Al–Mn system is not well established [14–16]. Although the phase diagram of Mg-rich corner in the Mg–Al–Mn ternary system has been thermodynamically assessed by Ohno et al. [17], the phase equilibria at lower temperatures were based on the constituents in the alloys solidified under practical casting conditions, which was far away from the thermodynamic equilibrium state. Therefore, it is necessary to experimentally determine a series of the isothermal sections in the Mg-rich corner so that the thermodynamic parameters can be well established, and then the microstructure constituents of an alloy with a certain composition can be predicted in the Mg–Al–Mn ternary system. The purpose of the present work is to determine the phase equilibria at 400 °C in the Mg–Al–Mn system by means of the equilibrated alloy method and diffusion couple technique in order to better understand the relationships among composition, microstructure and mechanical properties.

2. Experimental procedures

The desired alloys were prepared by using high purity Mg, Al, Mn (99.99 mass%) or Al–Mn master alloy, and their nominal compositions were list in the Table 1. The Mg–Al and Mg–Al–Mn alloys were melt in a high purity graphite crucible in the argon atmosphere using an induction furnace, and the Al–Mn master alloy were arc melt. Then the diffusion couple of the Mg–Al master alloy and Mn were prepared by using diffusion welding method. Finally, the diffusion couple and AM alloys were held at 400 °C for 446 or 672 h, and followed by water quenching.

The phase constituents of the heat treated alloys were determined by X-ray diffraction on a Philips PW3040/60 diffractometer. The microstructures and compositions of the diffusion couple and AM alloys were carried out on a Shimadzu EPMA-1610 Electron Probe Micro-analyzer.

3. Results and discussion

Fig. 1(a) shows the microstructure of the Mn/$Mg_{17}Al_{12}$ couple held at 400 °C for 446 h. A diffusion layer forms between the Mn metal and Mg–Al master alloy, and its thickness is about 10–15 μm. The concentration profiles, determined by EPMA, were illustrated

* Corresponding author. Tel.: +86 24 8368 3772; fax: +86 24 8368 6455.
E-mail address: qingw@smm.neu.edu.cn (G.W. Qin).

0925-8388/$ – see front matter © 2009 Elsevier B.V. All rights reserved.
doi:10.1016/j.jallcom.2009.01.008

Table 1
The nominal compositions of the desired alloys (at.%).

Alloy	Mg	Al	Mn
Mg–Al	55.0	45.0	–
Mg–Al–Mn	87.6	7.7	4.7
	85.6	9.7	4.7
	80.7	14.5	4.8
	65.6	29.6	4.8
Al–Mn	–	55.0	45.0

in the Fig. 1(b). According to the local equilibrium principle, the compositions of the equilibrium phases $Mg_{17}Al_{12}/Al_{11}Mn_4$ can be obtained, as listed in Table 2. It can be found that the solubility of Mn in the $Mg_{17}Al_{12}$ phase is very little, while the Mg can be dissolved in the $Al_{11}Mn_4$ compound phase, with a maximum solubility of about 1 at.%. However, no phases can be found between the Mn and $Al_{11}Mn_4$ phase, which is not in agreement with the Al–Mn binary phase diagram [18]. This is probably due to that the phases between the Mn and $Al_{11}Mn_4$ phase such as Al_8Mn_5 grow very slowly, while the $Al_{11}Mn_4$ phase very quickly. But it is interesting to find Al hardly passes across the $Al_{11}Mn_4$ phase into the Mn side to form the high-Al-content β-Mn phase.

In addition, there also exists the diffusion layer between the unmelted Mn and Mg matrix in the $Mg_{87.6}Al_{7.7}Mn_{4.7}$ alloy held at 400 °C for 672 h, and its microstructure and concentration profiles are shown in Fig. 2. Similar to the diffusion couple mentioned above, the phase compositions of the equilibrium phases α-Mn/β-Mn and β-Mn/α-Mg were also listed in Table 2. It can be seen from the results that the Mg can dissolve in the α-Mn and β-Mn phases

Table 2
The equilibrium phase constituents and compositions in the Mg–Al–Mn system at 400 °C.

Specimen	Equilibrium phase constituent	Equilibrium phase composition (at.%)		
		Mg	Al	Mn
$Mn/Mg_{17}Al_{12}$ couple	$Al_{11}Mn_4$	1.0	72.7	26.3
	$Mg_{17}Al_{12}$	57.6	42.0	0.4
Mn/Mg matrix couple	α(Mn)	1.1	14.2	84.7
	β(Mn)	2.6	30.7	66.7
Mn/Mg matrix couple	β(Mn)	0.3	36.4	63.3
	α-Mg	99.1	0.8	0.1
$Mg_{65.6}Al_{29.6}Mn_{4.8}$	α-Mg	90.9	9.1	0.0
	$Al_{11}Mn_4$	0.7	71.4	27.9
	$Mg_{17}Al_{12}$	62.5	37.5	0.0
$Mg_{80.7}Al_{14.5}Mn_{4.8}$	α-Mg	91.2	8.8	0.0
	$Al_{11}Mn_4$	0.6	71.1	28.3
	$Mg_{17}Al_{12}$	64.7	35.3	0.0
$Mg_{87.6}Al_{7.7}Mn_{4.7}$	α-Mg	96.1	3.9	0.0
	$Al_{11}Mn_4$	0.4	72.2	27.4
$Mg_{85.7}Al_{9.6}Mn_{4.7}$	α-Mg	94.2	5.7	0.1
	$Al_{11}Mn_4$	0.3	71.9	27.8

when the α-Mn phase is in equilibrium with the β-Mn phase. In contrast, the solubility of the Mg in the β-Mn phase is very little when the β-Mn phase is in equilibrium with the α-Mg phase. The contents of the Al in the equilibrium phases α-Mn and β-Mn are 14.2 and 30.7 at.%, respectively, which is apparently different from the phase boundary of α-Mn/β-Mn at 400 °C in the Al–Mn binary

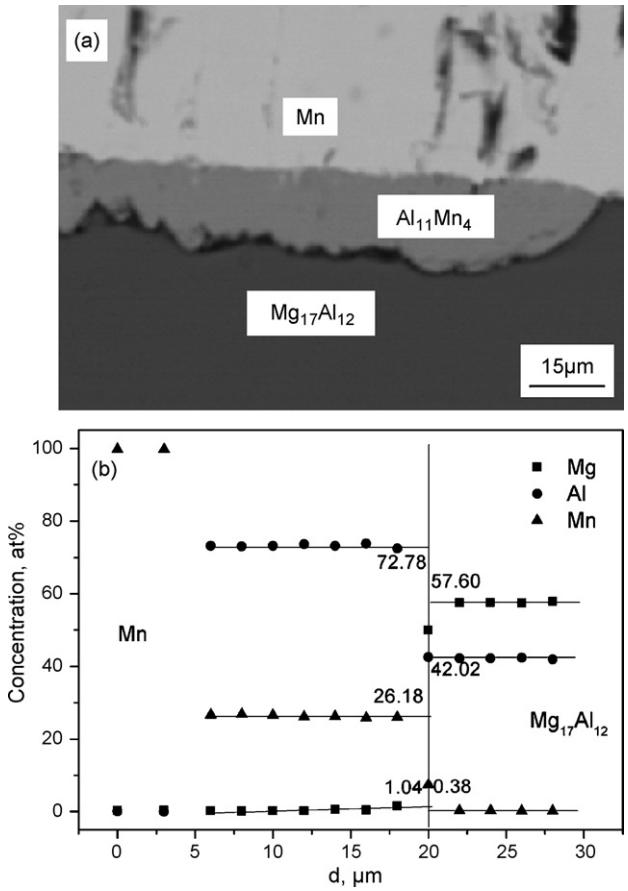

Fig. 1. The microstructure (a) and concentration profiles (b) of the $Mn/Mg_{17}Al_{12}$ couple held at 400 °C for 446 h.

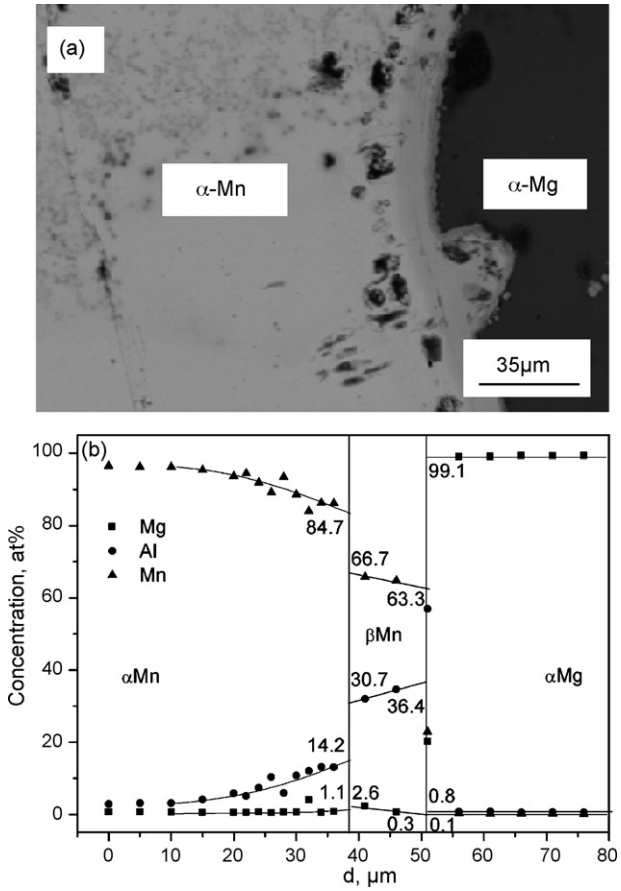

Fig. 2. The microstructure (a) and concentration profiles (b) of the unmelted Mn and Mg matrix couple in the $Mg_{87.6}Al_{7.7}Mn_{4.7}$ alloy held at 400 °C for 672 h.

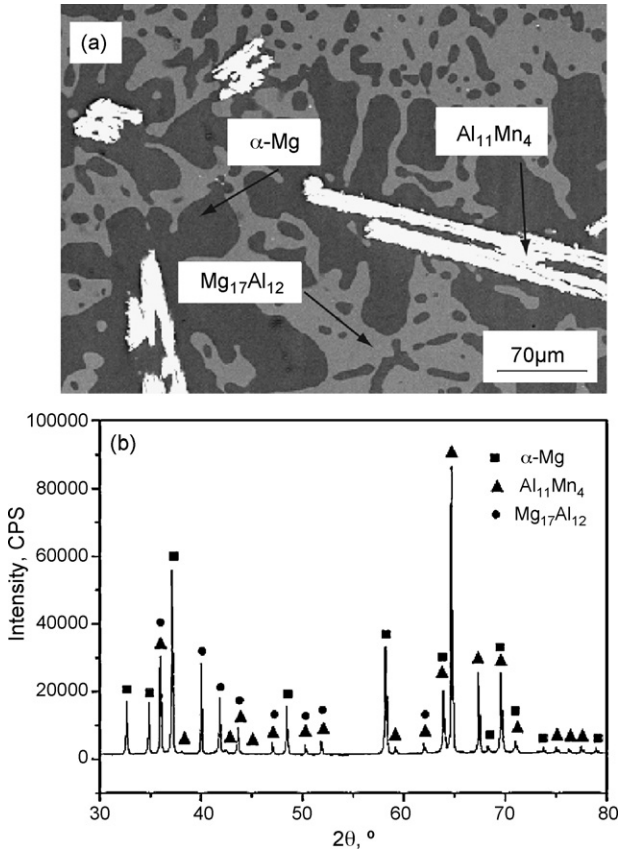

Fig. 3. The BSE image (a) and X-ray diffraction pattern (b) of the $Mg_{65.6}Al_{29.6}Mn_{4.8}$ alloy held at 400 °C for 672 h.

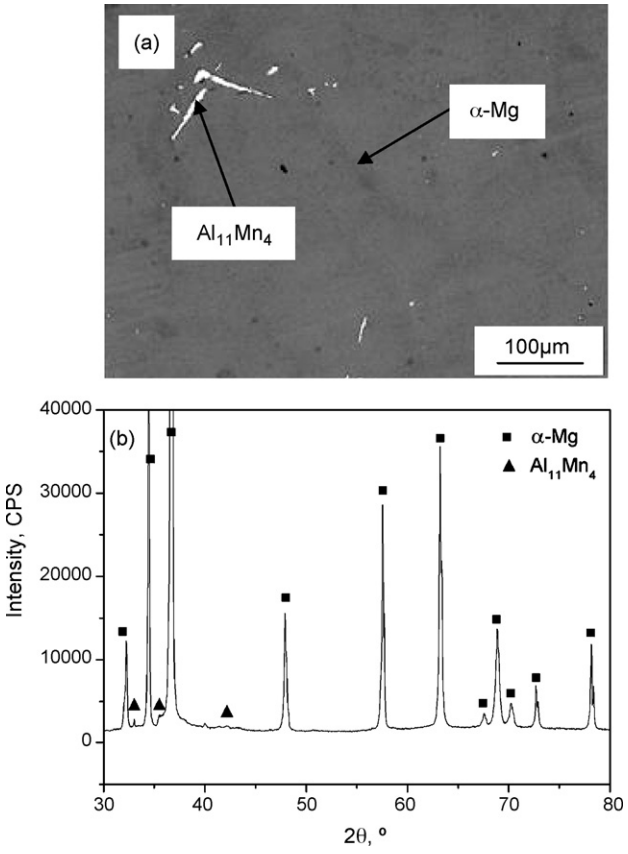

Fig. 4. The BSE image (a) and X-ray diffraction pattern (b) of the $Mg_{87.6}Al_{7.7}Mn_{4.7}$ alloy held at 400 °C for 672 h.

phase diagram [18]. Moreover, the solubility of the Al in the β-Mn phase is much higher when it is equilibrated with the α-Mg phase than that with the Al_8Mn_5 compound phase in the Al–Mn binary system [18].

The microstructures, equilibrium phase constituents and compositions in all designed alloys held at 400 °C for 672 h were carried out by means of SEM, XRD and EPMA, respectively. The typical microstructure and XRD pattern of the $Mg_{65.6}Al_{29.6}Mn_{4.8}$ alloy held at 400 °C for 672 h were shown in the Fig. 3. There are three equilibrium phases consisting of α-Mg, $Al_{11}Mn_4$ and $Mg_{17}Al_{12}$ phases. The compositions of the three phases were determined by using EPMA, as listed in the Table 2. The equilibrium phase constituents were also α-Mg, $Al_{11}Mn_4$ and $Mg_{17}Al_{12}$ phases in the $Mg_{80.7}Al_{14.5}Mn_{4.8}$ alloy held at 400 °C for 672 h, then the equilibrium phase compositions obtained by EPMA were also listed in the Table 2. It can be found that the solubilities of the Mn in both α-Mg and $Mg_{17}Al_{12}$ phases are very negligible. Moreover, the average contents Al in the $Mg_{17}Al_{12}$ phase is about 36.4 at.% when the α-Mg, $Al_{11}Mn_4$ and $Mg_{17}Al_{12}$ phases are in equilibrium, which is considerably different from that of the $Mg_{17}Al_{12}$ phase (about 41 at.%) in equilibrium with the α-Mg phase at 400 °C in the Mg–Al binary system [19].

Fig. 4 showed the backscattering electron (BSE) image and X-ray diffraction spectrum of the $Mg_{87.58}Al_{7.70}Mn_{4.72}$ alloy held at 400 °C for 672 h. There are two phases consisting of the dark matrix and light phase. It can be obtained by composition analysis that the dark phase is α-Mg solid solution and the light phase is $Al_{11}Mn_4$ compound, as shown in the Table 2. The amount of the $Al_{11}Mn_4$ compound is very small, which is also verified by X-ray diffraction spectrum (Fig. 4(b)). The diffraction peaks are mainly of the α-Mg solid solution. And the equilibrium phase constituents were also α-Mg and $Al_{11}Mn_4$ phases in the $Mg_{85.7}Al_{9.6}Mn_{4.7}$ alloy held at 400 °C for 672 h, then the equilibrium phase compositions obtained by EPMA were listed in Table 2.

Fig. 5 showed the changes of the X-ray diffraction peak positions of α-Mg solid solution in the four alloys held at 400 °C for 672 h. All the peaks clearly shift to the high diffraction angles due to the dissolution of Al in the α-Mg solid solution (Fig. 5(a)). This is because the atomic radius of the element Al is smaller than that of Mg. The peaks shift to the higher diffraction angle with increasing of the Al contents in the alloys (Fig. 5(b) and (c)). Moreover, the differences of the diffraction angles between the alloys and pure Mg also increase with the increasing of the diffraction angle, which increasingly appear linear (Fig. 5(c)). The maximum solubility of Al in the α-Mg phase reaches ~9.0 at.% when the α-Mg/$Mg_{17}Al_{12}$/$Al_{11}Mn_4$ three phases are in equilibrium at 400 °C. Cohen least squares method [20] was adopted to determine the lattice parameters dependency of the α-Mg solid solution on the Al content in the Mg–Al–Mn ternary system, according to the X-ray diffraction results of the four alloys held at 400 °C (Fig. 5), as shown in Fig. 6. The solute Al has smaller atomic size as compared to Mg, which thus causes a contraction of lattice both in a and c values as the solute Al concentration increases (Fig. 6). The a and c values of α-Mg do not appear linear with the Al content, which is a little different from the results of Nayeb-Hashemi et al. [21] or park et al. [22] who used Mg–Al binary alloys. This is possibly due to the small amount of Mn in the α-Mg solid solution.

According to the equilibrium phase constituents and compositions obtained above, the isothermal section of the Mg–Al–Mn system at 400 °C was finally illustrated in the Fig. 7. Besides the $Mg_{17}Al_{12}$ phase, the phase equilibria with the α-Mg phase at 400 °C are the Al–Mn phases, such as the β-Mn, Al_8Mn_5 and $Al_{11}Mn_4$. The (α-Mn + β-Mn) two-phase region in the Mg–Al–Mn system

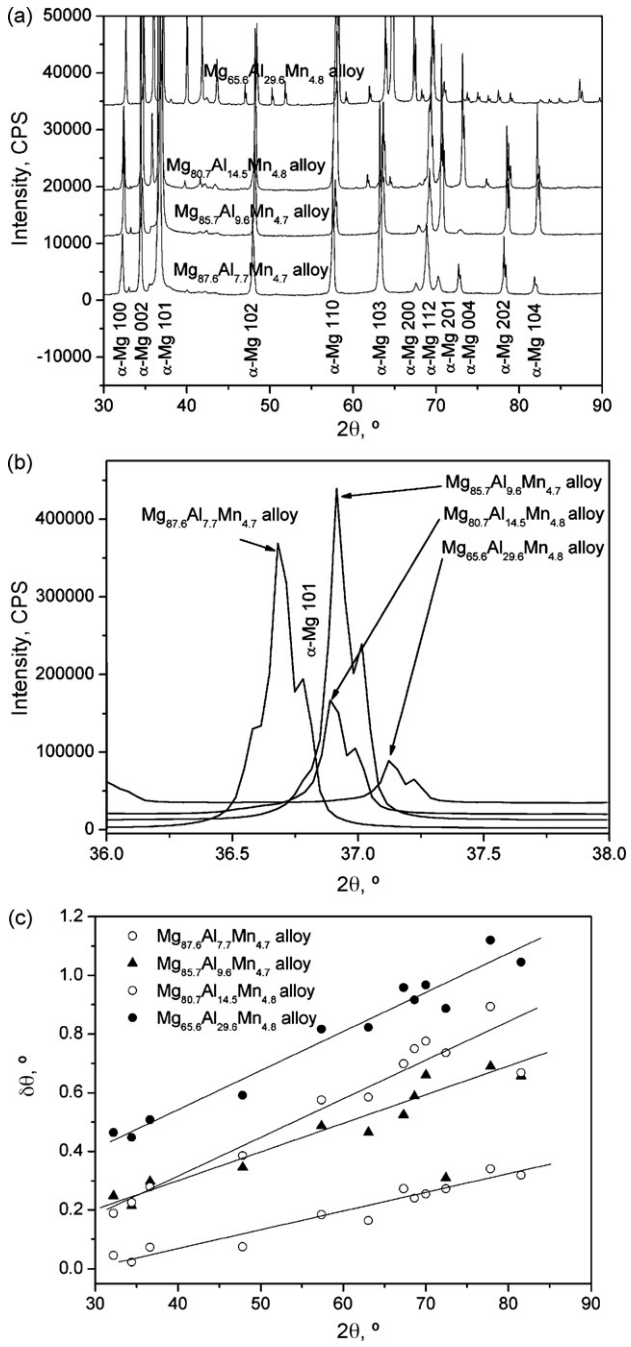

Fig. 5. XRD diffraction patterns of the four alloys treated at 400 °C for 672 h: (a) diffraction patterns of the four alloys, (b) higher magnification of XRD patterns at 2θ of 36.0–38.0 and (c) the changes of the diffraction angle difference between the treated alloys and pure Mg.

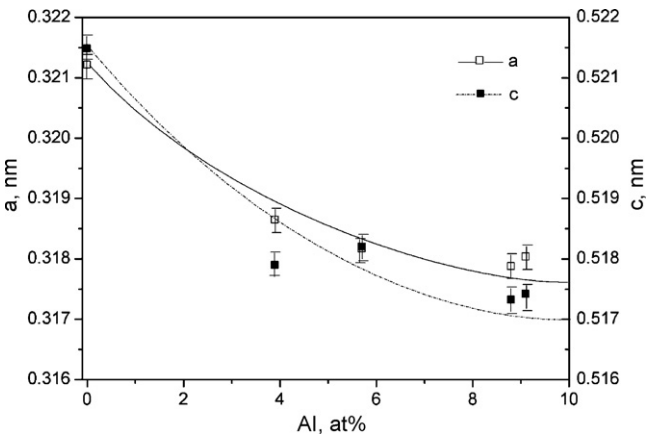

Fig. 6. The lattice parameters dependence of the α-Mg phase on Al content in the Mg–Al–Mn ternary system.

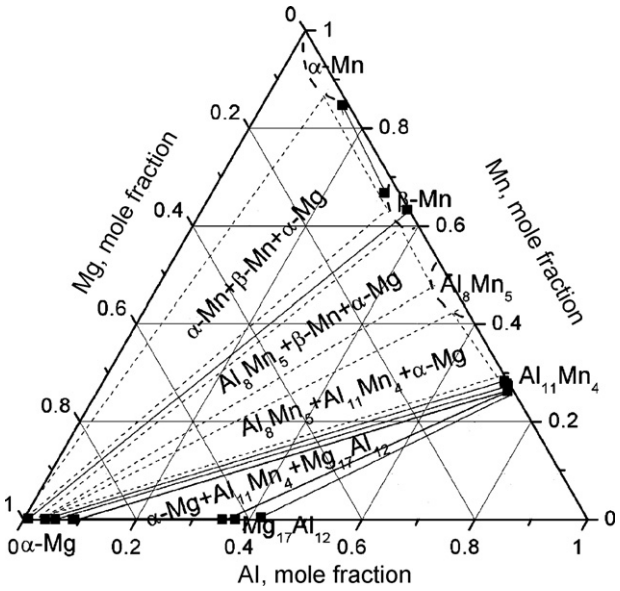

Fig. 7. Isothermal section of the Mg-rich corner in the Mg–Al–Mn ternary system at 400 °C.

becomes wider and shifts to the Al-rich side, compared to the currently accepted Al–Mn binary system [18]. So far, the experimental work on the Al–Mn binary phase diagram has been mainly focused on the Al side and Mn side at high temperatures, and the phase diagram in the Mn-rich side at lower temperatures was obtained by thermodynamic calculation [23,24]. Therefore, it is necessary to experimentally determine the Al–Mn phase diagram in the Mn-rich side at lower temperatures in the future in order to rightly assess the thermodynamic parameters of the Mg–Al–Mn ternary system. On the other hand, the Al content of the $Mg_{17}Al_{12}$ phase in equilibrium with the α-Mg phase is about 40 at.% Al in the presently accepted Mg–Al binary phase diagram, while it is around 36 at.% Al in the present work. Therefore, the current Mg–Al binary phase diagram should also be determined experimentally and re-assessed thermodynamically in the future in order to get a reasonable Mg–Al–Mn ternary phase diagram.

From the present isothermal section at 400 °C, the Al_8Mn_5, Al_6Mn, $Al_{86}Mn_{14}$ or Al_4Mn compounds were metastable in the commercial AM50 Mg alloy treated at 400 °C for short time in literature [6,8]. If prolonging heat treatment time, there should be only equilibrium phases consisting of the α-Mg matrix and $Al_{11}Mn_4$ compound. Besides, the $Mg_{17}Al_{12}$ phase can be suppressed and the strengthened phases can be modified into the Al–Mn phases if the Mn content in the AM series alloys is increased to some extent. Since the Al–Mn phases are very stable at elevated temperatures, it is thus expected to improve creep resistance of the AM series Mg alloys through this cost-effective microstructure control.

4. Conclusions

The isothermal section in the Mg-rich corner of the Mg–Al–Mn ternary system at 400 °C has been determined. It is found that the phases equilibrated with the α-Mg phase are the $Mg_{17}Al_{12}$ phase and the Al–Mn phases such as the β-Mn, Al_8Mn_5 and $Al_{11}Mn_4$

at 400 °C. No ternary compounds were detected in the Mg-rich corner at this temperature. Moreover, the solubility of Mn in the phases α-Mg and $Mg_{17}Al_{12}$ was very little. And the element Mg can slightly dissolve in the compound $Al_{11}Mn_4$. There is some difference in phase equilibrium compositions of Mg–Al–Mn system between the present data and accepted Mg–Al and Al–Mn binary systems, especially at low temperatures, which is thus needed to be further investigated in order to establish the appropriate thermodynamic parameters of the Mg–Al based alloy systems. Also, the lattice parameter dependence of α-Mg solid solution on Al content in Mg–Al–Mn system was finally determined by the XRD results.

Acknowledgements

The work was supported by "115" National Key Technology R&D Program (No. 2006BAE04B09-7), Shenyang Talents Supporting Program (No.2007010303025), Key Project of National Natural Science Foundation of China (No. 50731002) and A Canada-China-USA Collaborative Research & Development Project (2007DFB50150-10)

References

[1] B.L. Mordike, T. Ebert, Mater. Sci. Eng. A 302 (2001) 37–45.
[2] S. Ji, M. Qian, Z. Fan, Metall. Mater. Trans. A 37 (2006) 779–787.
[3] M. Tiryakioğlu, Mater. Sci. Eng. A 465 (2007) 287–289.
[4] Y. Terada, N. Ishimatsu, Y. Mori, T. Sato, Mater. Trans. 46 (2005) 145–147.
[5] S.G. Lee, G.R. Patel, A.M. Gokhale, A. Sreeranganathan, M.F. Horstemeyer, Scripta Mater. 53 (2005) 851–856.
[6] J. Medved, P. Mrvar, Mater. Sci. Forum 508 (2006) 603–608.
[7] Y.Q. Liu, A. Das, Z. Fan, Mater. Sci. Technol. 20 (2004) 35–41.
[8] Y.L. Ma, J. Zhang, M.B. Yang, J. Alloys Compd. (2008), doi:10.1016/j.jalcom.2008.03.047.
[9] E. Gariboldi, A. Lo Conte, Mater. Sci. Eng. A 387–389 (2004) 34–40.
[10] M. Zhou, H. Hu, N.Y. Li, J. Lo, J. Mater. Eng. Perform. 14 (2005) 539–545.
[11] P. Cao, M. Qian, D.H. StJohn, Scripta Mater. 54 (2006) 1853–1858.
[12] M.X. Zhang, P.M. Kelly, M. Qian, J.A. Taylor, Acta Mater. 53 (2005) 3261–3270.
[13] T. Motegi, E. Yano, Y. Tamura, E. Sato, Mater. Sci. Forum 350–351 (2000) 191–199.
[14] V. Raghavan, J. Phase Equilib. Diffus. 28 (2007) 201–202.
[15] C.J. Simensen, B.C. Oberländer, J. Svalestuen, A. Thorvaldsen, Z. Metall. 79 (1988) 696–699.
[16] W. Matienssen, in: G. Effenberg, S. Ilyenko (Eds.), Ternary alloy Systems—Phase Diagrams, Crystallographic and Thermodynamic Data, Springer, Germany, 2006, pp. 142–147.
[17] M. Ohno, R. Schmid-Fetzer, Z. Metall. 96 (2005) 857–869.
[18] H. Okamoto, J. Phase Equilib. 15 (1994) 123–124.
[19] J.L. Murray, in: T.B. Massalski (Ed.), Al–Mg Phase Diagram, ASM International, Materials Park, OH, 1990, pp. 169–171.
[20] M.U. Cohen, Rev. Sci. Instrum. 6 (1935) 68–73.
[21] A.A. Nayeb-Hashemi, J.B. Clark, Phase Diagrams of Binary Magnesium Alloys, ASM International, Metals Park, 1988.
[22] J.S. Park, Y.W. Chang, Adv. Mater. Res. 26–28 (2007) 95–98.
[23] X.J. Liu, I. Ohnuma, R. Kainuma, K. Ishida, J. Phase Equilib. 20 (1999) 45–56.
[24] Y. Du, J. Wang, J. Zhao, J. Schuster, F. Weitzer, R. Schmid-Fetzer, M. Ohno, H. Xu, Z. Liu, S. Shang, W. Zhang, J. Mater. Res. 98 (2007) 855–871.